CELL STRUCTURE AND FUNCTION 41: 1–11 (2016)

Yeast Ivy1p Is a Putative I-BAR-domain Protein with pH-sensitive Filament Forming Ability *in vitro*

Yuzuru Itoh[1*], Kazuki Kida[2], Kyoko Hanawa-Suetsugu[1,2], and Shiro Suetsugu[1,2]**

[1]*Laboratory of Membrane and Cytoskeleton Dynamics, Institute of Molecular and Cellular Biosciences, The University of Tokyo, 1-1-1 Yayoi, Bunkyo-ku, Tokyo 113-0032, Japan,* [2]*Laboratory of Molecular Medicine and Cell Biology, Graduate School of Biosciences, Nara Institute of Science and Technology, Ikoma 630-0192, Japan*

ABSTRACT. **Bin-Amphiphysin-Rvs161/167 (BAR) domains mold lipid bilayer membranes into tubules, by forming a spiral polymer on the membrane. Most BAR domains are thought to be involved in forming membrane invaginations through their concave membrane binding surfaces, whereas some members have convex membrane binding surfaces, and thereby mold membranes into protrusions. The BAR domains with a convex surface form a subtype called the inverse BAR (I-BAR) domain or IRSp53-MIM-homology domain (IMD). Although the mammalian I-BAR domains have been studied, those from other organisms remain elusive. Here, we found putative I-BAR domains in Fungi and animal-like unicellular organisms. The fungal protein containing the putative I-BAR-domain is known as Ivy1p in yeast, and is reportedly localized in the vacuole. The phylogenetic analysis of the I-BAR domains revealed that the fungal I-BAR-domain containing proteins comprise a distinct group from those containing IRSp53 or MIM. Importantly, Ivy1p formed a polymer with a diameter of approximately 20 nm *in vitro*, without a lipid membrane. The filaments were formed at neutral pH, but disassembled when pH was reverted to basic. Moreover, Ivy1p and the I-BAR domain expressed in mammalian HeLa cells was localized at a vacuole-like structure as filaments as revealed by super-resolved microscopy. These data indicate the pH-sensitive polymer forming ability and the functional conservation of Ivy1p in eukaryotic cells.**

Key words: I-BAR domain, IMD, BAR domain, polymerization

Introduction

The BAR-domain containing proteins (BAR proteins), which form the BAR protein superfamily, mold amorphous lipid bilayer membranes into defined tubular shapes by their rigid protein folds (Daumke *et al.*, 2014; Doherty and McMahon, 2008; Suetsugu *et al.*, 2014). The BAR domain has a surface rich in positively charged amino-acid residues. The interaction of these positively charged amino-acid residues with the negatively charged membrane lipids is thought to drive the generation or sensing of membrane curvature. Three subtypes of BAR domains, the canonical BAR, F-BAR, and I-BAR domains, are included in the superfamily (Daumke *et al.*, 2014; Doherty and McMahon, 2008; Suetsugu *et al.*, 2014). The canonical BAR and F-BAR domains are considered to be involved in forming membrane invaginations, such as clathrin-coated pits and caveolae (Daumke *et al.*, 2014; Doherty and McMahon, 2008; Suetsugu *et al.*, 2014). The canonical BAR and F-BAR domains have a concave membrane binding surface, which enables the formation of a spiral polymer on the surface of the plasma membrane invagination or the membrane tubulation of liposomes *in vitro*. An exception is the F-BAR domains of srGAPs, which reportedly formed cellular protrusions upon overexpression (Guerrier *et al.*, 2009; Suetsugu and Gautreau, 2012). However, it remains unclear whether the F-BAR domains of srGAPs contribute to the protrusive membrane structures, because their crystal struc-

*Present address: Yuzuru Itoh, Institut de Génétique et de Biologie Moléculaire et Cellulaire, 1 rue Laurent Fries, 67400 Illkirch-Graffenstaden, France.

**To whom correspondence should be addressed: Shiro Suetsugu, Laboratory of Molecular Medicine and Cell Biology, Graduate School of Biosciences, Nara Institute of Science and Technology, Ikoma 630-0192, Japan.
Tel: +81–743–72–5430, Fax: +81–743–72–5439
E-mail: suetsugu@bs.naist.jp

Abbreviations: BAR, Bin-Amphiphysin-Rvs161/167; I-BAR, inverse BAR; IMD, IRSp53-MIM-homology domain.

tures have not been reported.

The I-BAR domains were initially characterized as the IRSp53-MIM-homology domain (IMD). The I-BAR domains have convex membrane-binding surfaces that correspond to the inner surface of plasma membrane protrusions (Scita *et al.*, 2008; Suetsugu *et al.*, 2006). The convex membrane-binding surface allows the I-BAR domain to reside on the inner surface of the membrane tubule. The I-BAR domain also reportedly forms a spiral polymer on the inner surface of the tubules, thereby promoting the formation of membrane protrusions (Mattila *et al.*, 2007; Saarikangas *et al.*, 2009).

Cellular protrusions are prominent in cells from multicellular organisms, but are less frequently observed in unicellular organisms. In this study, we extensively investigated the amino-acid sequences in fungal genomes, and found a putative I-BAR domain in Fungi, including the yeast *Saccharomyces cerevisiae*.

Materials and Methods

Protein expression and purification

The DNA sequences encoding the full-length Ivy1p (1–453 aa) and its I-BAR domain (87–325 aa) from the yeast *S. cerevisiae* were cloned into the vectors pCold II (Takara), through the BamH I and Sal I restriction sites, to include an N-terminal affinity tag (His_6). The *Escherichia coli* strain JM109 was transformed by the expression plasmid, and the protein was overexpressed in LB medium at 15°C. The harvested *E. coli* cells were re-suspended in the buffer, containing 20 mM Tris-HCl (pH 7.5), 0.5 M NaCl, 0.5 M $MgCl_2$, 20% glycerol, 1 mM 2-mercaptoethanol, and 1 mM phenylmethanesulfonyl fluoride (PMSF), and were disrupted with an ultrasonic homogenizer. The lysate was centrifuged, and the solubility of the proteins was analyzed. The His_6-tagged full-length Ivy1p was purified for *in vitro* analyses. The supernatant of the lysate was loaded on a Ni-Sepharose 6 Fast Flow column (GE Healthcare). The column was extensively washed with buffer containing 20 mM Tris-HCl (pH 8.5), 0.7 M NaCl, 20 mM imidazole, and 1 mM PMSF. And the protein was eluted with the buffer containing 20 mM Tris-HCl buffer (pH 8.5) and 0.7 M NaCl supplemented with 0.8 M imidazole, with the overall pH 9.5, resulting in the "purified Ivy1p".

Gelation of Ivy1p

Purified Ivy1p (16.9 μM) were dialyzed in PBS (pH 7.4) containing 10 mM 2-mercaptoethanol and 0.2 mM PMSF, and then the gelation was examined by pelleting after centrifugation at 20,400×g for 5 min. For resolubilization of the gelled filaments, the pellet was re-suspended in PBS containing 0.6 M imidazole or 0.1 M Tris (the final pH values are 9.0 and 9.5, respectively), incubated at room temperature for 20 mins, and then analyzed by centrifugation. The pH was monitored by pH indicator paper.

Electron microscopy

The purified Ivy1p (16.9 μM) or its filaments Ivy1p after dialysis in PBS was diluted in 10-fold in PBS for observing filaments, while the purified Ivy1p (16.9 μM) was diluted in 10 mM Tris without pH adjustment for observing solubilized Ivy1p. The high concentrations of NaCl, imidazole and Tris prevent the observation under EM by negative staining. These Ivy1p solutions were applied to glow-discharged collodion- and carbon-coated copper grids for 1 min, which were washed in 100 mM Hepes-NaOH (pH 7.9). The grids were then negatively stained with 0.5% uranyl acetate for 1 min. At each step, excess solution was removed with a filter paper. The dried grids were examined using an electron microscope.

HeLa cell culture

HeLa cells were cultured in Dulbecco's Modified Eagle Medium, supplemented with 10% fetal bovine serum (Senju *et al.*, 2011). Transfection was performed with the Lipofectamine LTX and PLUS reagents (Invitrogen), according to the manufacturer's recommendations, and cells were observed using a confocal microscope (Olympus FV1000D).

Super resolved microscopy

The stochastic optical reconstruction microscopy (STORM) setup was obtained from Nikon, which was developed based on previous reports (Bates *et al.*, 2007; Huang *et al.*, 2008). The nanobody against GFP was purified and labeled with Alexa 647 according to the manufacturer's instruction (Katoh *et al.*, 2015; Ries *et al.*, 2012). Cells were cultured on glass-bottomed dishes, and were fixed in 3% paraformaldehyde+0.1% glutaraldehyde (electron microscopy grade) in HEPES-buffered saline for 10 min, blocked in blocking buffer (3% BSA+0.2% Triton X-100 in PBS) for 1 hr, and then stained with 0.14 μg/ml Alexa647-labelled nanobody in blocking buffer for 1 hr. After washing with PBS, the cells were observed. During STORM observation, the cells were with 0.1 M cystamine. Forty thousands of images were acquired continuously with 647 nm laser and each single molecule localization was analyzed with the software provided by Nikon.

Results

Identification of putative I-BAR proteins in Fungi

The BAR domains of the superfamily proteins lack amino-acid sequence similarity. For example, the canonical BAR and I-BAR domains have approximately 250 amino-acid residues, whereas the F-BAR domains have approximately 300 amino-acid residues. The basic local alignment search tool (BLAST) (Altschul *et al.*, 1997) used with the standard setting does not readily find any I-BAR or F-BAR proteins, using the amino-acid sequence of a canonical BAR domain,

such as that of amphiphysin. The BLAST search using the I-BAR domains of mammalian IRSp53 and MIM did not detect any I-BAR proteins in Fungi.

The I-BAR domain was first described in mammals. Mammals belong to the Animalia/Metazoa kingdom, within the Eukaryota domain (Adl *et al.*, 2012; Cavalier-Smith, 2009; Shalchian-Tabrizi *et al.*, 2008). In the Eukaryota domain, the Animalia, Choanoflagellates, Filasterea, Ichthyosporea, Fungi, and Nucleariidae kingdoms form a broader group called the Opsithokonts (Maddison and Schulz, 2009; Maddison *et al.*, 2007), in which the Animalia, Choanoflagellates, and Filasterea are relatively close to each other. We expected that the I-BAR-domain containing proteins (I-BAR proteins) from Filasterea and Choanoflagellates could be useful to search for fungal I-BAR proteins. However, no I-BAR protein was identified in these groups.

Therefore, we first searched the I-BAR proteins of *Capsaspora owczarzak* from Filasterea (Suga *et al.*, 2013) and *Salpingoeca rosetta* from Choanoflagellates (Fairclough *et al.*, 2013), which are both animal-like, unicellular organisms. By a BLAST search using human MIM as a query, four putative I-BAR proteins (RefSeq IDs: XP_004365908.1, XP_004349890.2, XP_004363741.1, XP_004365185.1) were found in *Capsaspora owczarzak*, with E values of 5e-24, 2e-21, 1e-08, and 9e-05, respectively. Using the I-BAR-containing region (residues 1–280) of XP_004365908.1 as a query, a protein from the fungus *Colletotrichum graminicola* (RefSeq ID: XP_008096771.1) was detected, with an E-value of 1e-05.

The conserved domain search tool from NCBI (Marchler-Bauer *et al.*, 2015) predicted the presence of a BAR domain (residues 58–210) in the fungal protein XP_008096771.1, suggesting that this protein is a putative I-BAR protein. A further BLAST search on fungal proteins revealed that this protein is conserved in Fungi, including *Zygosaccharomyces rouxii*, *Ogataea parapolymorpha*, *Yarrowia lipolytica*, *Ustilago maydis*, *Cryptococcus gattii*, *Schizophyllum commune*, *Laccaria bicolo*r, and *S. cerevisiae* (Fig. 1A). The orthologue in *S. cerevisiae* was named Ivy1p, and was already known to be localized at vacuole and to bind phospholipids, without strong specificity to particular phospholipids (Lazar *et al.*, 2002).

Phylogenic analyses of the I-BAR proteins

We performed a phylogenic analysis to compare the putative I-BAR domain of Ivy1p to other I-BAR domains, using the Clustal X program (Fig. 1A and Fig. 2). Based on the amino-acid sequence homology of the I-BAR domain regions, the I-BAR proteins are divided into three groups: the IRSp53 I-BAR, MIM I-BAR, and fungal I-BAR groups (Fig. 1A). The IRSp53 I-BAR group only consists of animal I-BAR proteins, including three vertebrate paralogues, IRSp53/BAIAP2, IRTKS/BAIAP2L1, and Pinkbar/BAIAP2L2, and related proteins from other animals, such as insects and the simple multicellular organism *Trichoplax adhaerens* (Fig. 1A). The MIM I-BAR group has two vertebrate paralogues, MIM/MTSS1 and ABBA-1/MTSS1L, and closely related proteins from other animals. Interestingly, the members of Amoebozoa, including *Dictyostelium discoideum*, *Dictyostelium purpureum*, and *Polysphondylium pallidum*, do not belong to the Opsithokonts, but their I-BAR proteins belong to the MIM I-BAR group. The I-BAR proteins of *Capsaspora owczarzak* from Filasterea and *Salpingoeca rosetta* from Choanoflagellates also belong to the MIM I-BAR group (Fig. 1A). In contrast, the fungal I-BAR group only consists of fungal proteins (Fig. 1A).

In the alignment, the most important amino-acid residues for lipid binding, such as K146 and K147 of human IRSp53 (Suetsugu *et al.*, 2006), appeared to be mostly conserved as basic-charged amino-acid residues in fungal I-BAR domains (Fig. 2). Furthermore, secondary structure prediction indicates similar helix compositions of fungal I-BAR domains compared to those of the other known I-BAR domains (Fig. 2).

We then compared the amino-acid sequences of the I-BAR domains of these three groups to those of the canonical BAR and F-BAR domains (Fig. 1B). The fungal I-BAR protein Ivy1p is not present on any branches of the canonical BAR and F-BAR proteins, and is relatively closer to the known I-BAR proteins. Thus, the fungal I-BAR protein may represent a new subtype of the BAR protein superfamily that is closer to IRSp53 and MIM.

Domain architecture of the I-BAR proteins

We examined the domain architecture of these I-BAR proteins, using the Simple Modular Architecture Research Tool (SMART) (Fig. 3) (Letunic *et al.*, 2015). The fungal I-BAR proteins do not have any other putative domains, based on the SMART analysis. However, the IRSp53 I-BAR group proteins contain an SH3 domain. The SH3 domains from the BAR superfamily proteins often bind to the proline-rich regions of WASP family proteins and dynamin, which function in actin polymerization and membrane scission (Takenawa and Suetsugu, 2007). The domain architectures of the MIM I-BAR group proteins are heterogeneous. The I-BAR proteins from Amoebozoa contain an SH3 domain, while some proteins in the Animal kingdom contain the WH2 domain, which is a ~35 residue actin monomer binding motif (Paunola *et al.*, 2002). Several MIM I-BAR group proteins have no other domain. However, because the amino-acid conservation in WH2 domain is weak, it is possible that the SMART search could not find potential WH2 domains (Paunola *et al.*, 2002). Only the protein from *Polysphondylium pallidum* (EFA83649.1) contains the membrane-binding domain (Pfam ID: PF14564) found in calcium-dependent cell adhesion mole-

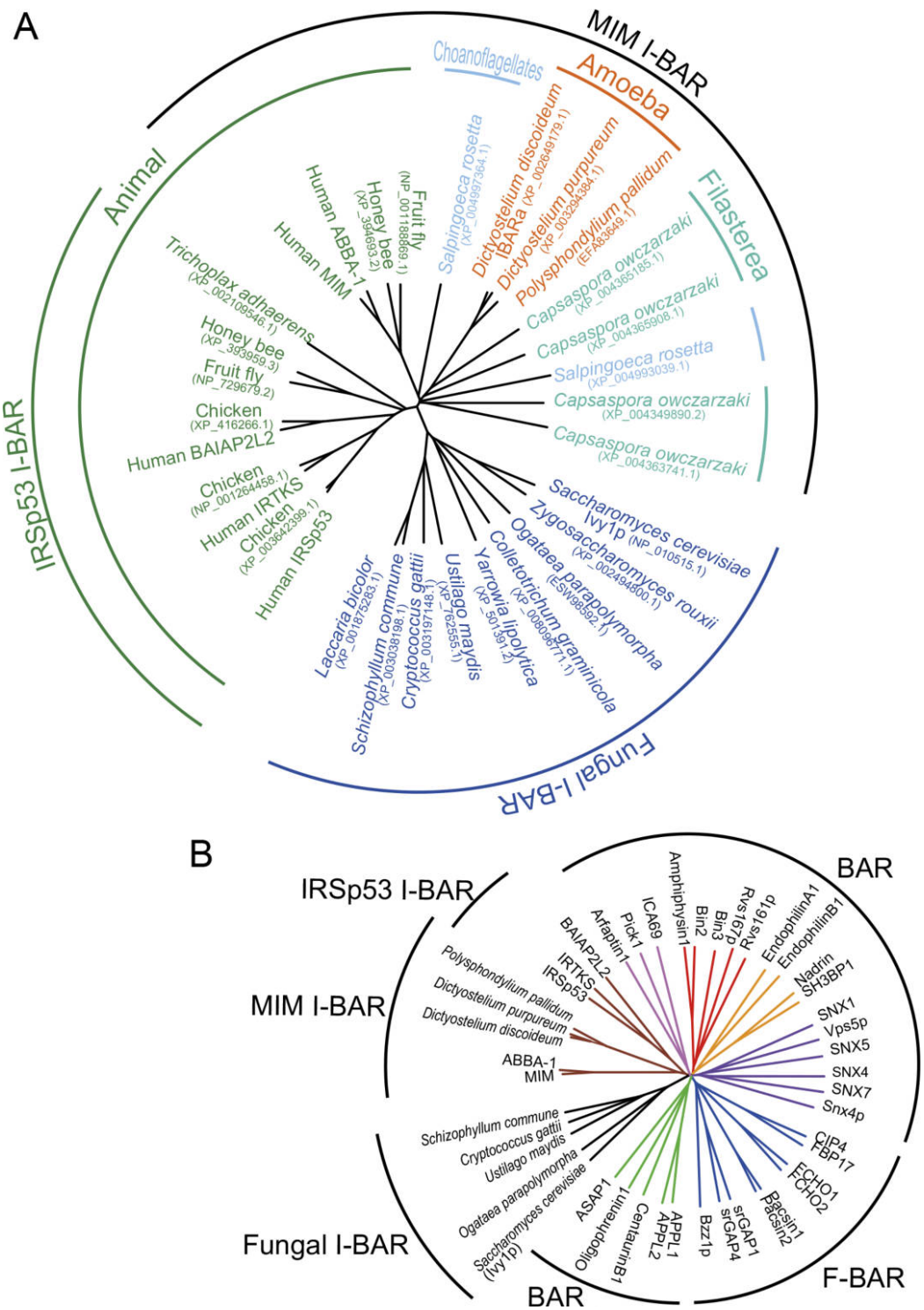

Fig. 1. Phylogenetic analysis of I-BAR proteins. (A) The amino-acid sequences of the I-BAR domain containing regions of Ivy1ps, known I-BAR proteins, and putative I-BAR proteins from animal-like unicellular organisms were compared to make a phylogenic tree, using the Clustal X program (Larkin *et al.*, 2007). (B) Fungal I-BAR proteins, amoeba I-BAR proteins, and representative human and *S. cerevisiae* BAR proteins were compared. The amino-acid sequences of their BAR, I-BAR, and F-BAR domains were used to make the phylogenic tree.

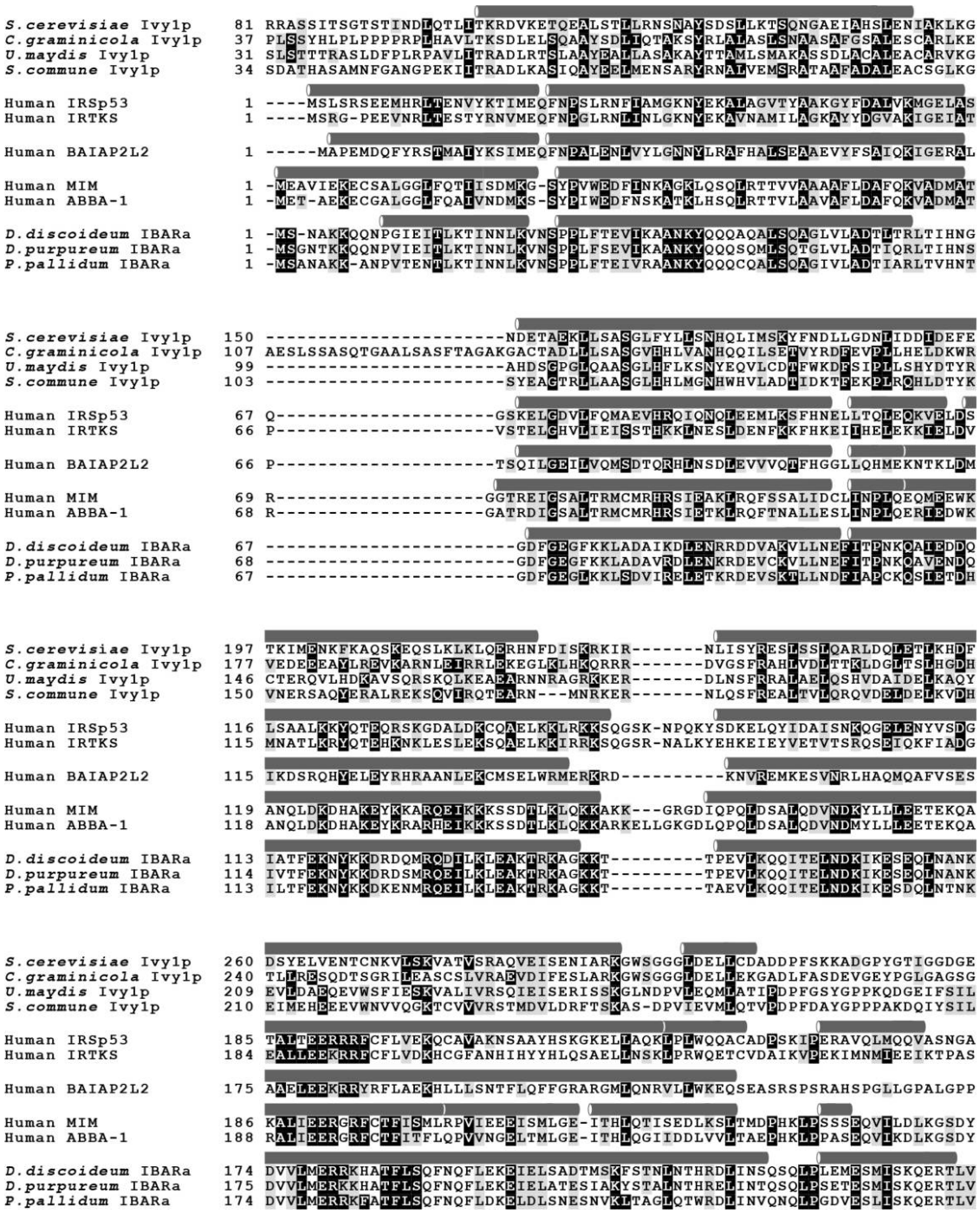

Fig. 2. Sequence alignment of I-BAR domains. The amino-acid sequences of representative I-BAR domains were aligned by Clustal X program (Larkin *et al.*, 2007), followed by revision based on the reported crystal structures of IRSp53 (Millard *et al.*, 2007; Suetsugu *et al.*, 2006), Pinkbar/BAIAP2L2 (Pykalainen *et al.*, 2011), MIM (Lee *et al.*, 2007), and IBARa (Linkner *et al.*, 2014). The alignment was exhibited by using BoxShade program. The secondary structure of *S. cerevisiae* Ivy1p was predicted by Psipred program (Buchan *et al.*, 2013) and illustrated along with the sequences. The cylinders represent helices and no β sheet was found in the prediction. The secondary structures of known I-BAR domains, generated from their crystal structures, are also shown for comparison.

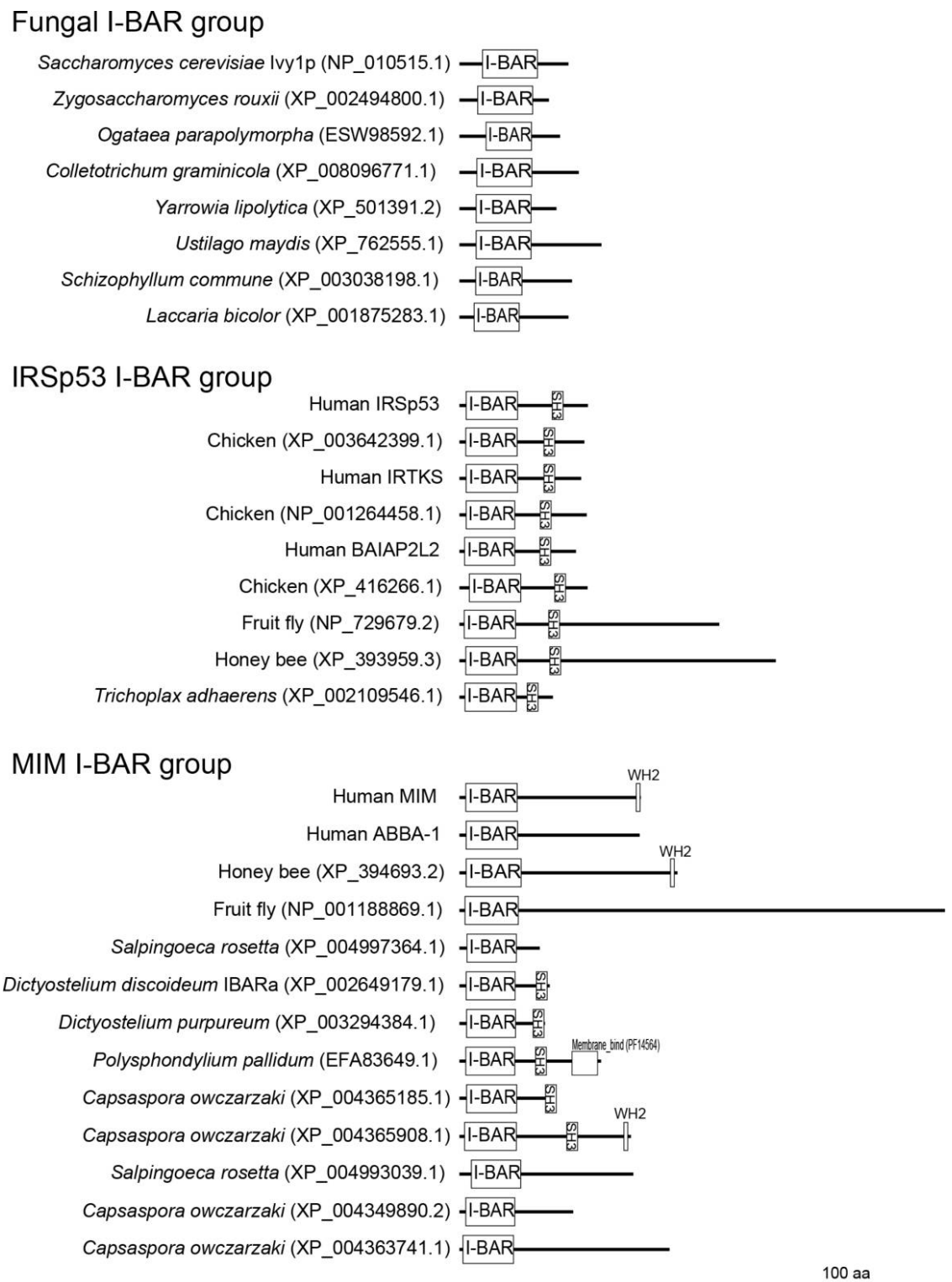

Fig. 3. Domain composition of proteins with I-BAR domains. The domains were predicted by SMART (Letunic *et al.*, 2015). The bar indicates the length of 100 amino-acid residues.

cule 1 (P54657) of *Dictyostelium discoideum*, which has an immunoglobulin-like fold that tethers the protein to the cell membrane (Lin *et al.*, 2006).

Polymer formation of Ivy1p

We examined the characteristics of the fungal I-BAR protein, using the *S. cerevisiae* Ivy1p. We expressed the I-BAR-domain containing fragment (87–325 aa) and the full-length Ivy1p (1–453 aa) in *E. coli* (Fig. 4A). Since the His_6-tagged I-BAR domain fragment was present in the insoluble fraction, we could not purify this fragment (Fig. 4B). In contrast, the His_6-tagged full-length Ivy1p was expressed and solubilized (Fig. 4B). The His_6-tagged Ivy1p was successfully purified by elution with imidazole from a nickel affinity column. Interestingly, when dialyzed against PBS or diluted in PBS, Ivy1p turned to be gelatinous, and was observed as a precipitate after centrifugation (Fig. 4C).

To determine whether the gelled protein was generated by aggregation or polymer formation, the purified protein and the gelled protein was observed by electron microscopy after negative staining with uranium acetate (Fig. 4D and E). The results revealed that the gelled protein did not result from protein aggregation, but was the product of filamentous polymer formation (Fig. 4E), whereas the protein appeared to be purified as monomers or small oligomers, which we could not be distinguished by the electron microscopic analysis (Fig. 4D). The diameter of the Ivy1p polymer was approximately 20 nm (Fig. 4F).

We then speculated that the lowering pH from basic to neutral induced the gelation. If this hypothesis is correct, then the polymer formation was supposed to be sensitive to pH. Then we added elevated the pH of buffer containing the gelled Ivy1p. Elevation of the pH to basic conditions by adding higher concentration of imidazole or Tris reverted the gelation and resolubilized Ivy1p, observed as the protein in the supernatant after centrifugation (Fig. 4C). Therefore, the filaments polymer formation of Ivy1p is dependent on pH and reversible.

The intracellular localization of Ivy1p in HeLa cells

Ivy1p is known to function in the vacuole in *S. cerevisiae*. To examine the conservation of the function, we expressed Ivy1p as a GFP-fusion protein in HeLa cells. The prominent localization of Ivy1p in the vacuole-like structure was observed (Fig. 5). The I-BAR domain alone fused with GFP was localized similarly in HeLa cells, whereas such localization was not observed with GFP alone, indicating that the I-BAR domain was responsible for vacuole localization (Fig. 5). To examine the filament formation of Ivy1p, GFP-Ivy1p was observed using STORM, where GFP was labeled with nanobody conjugated with Alexa647. The Alexa647 signals were stochastically obtained to reconstitute the super-resolved images of GFP-Ivy1p localization (Fig. 6). The reconstituted images indicated the filamentous structure of the expressed Ivy1p and its I-BAR domain around the vacuole-like structures.

Discussion

The I-BAR domain was first characterized as a subtype of the BAR domain (Mattila *et al.*, 2007; Suetsugu *et al.*, 2006). The I-BAR proteins IRSp53 and MIM localize at filopodia through their I-BAR domains, but membranes with the same topology are also found among intracellular membranes, such as those of vacuole. Interestingly, the *Dictyostelium discoideum* I-BAR protein, IBARa, was reported to be localized at the vacuole (Linkner *et al.*, 2014), while IBARa is also found at the leading edge and protrusions (Linkner *et al.*, 2014; Veltman *et al.*, 2011). The fungal I-BAR protein, Ivy1p, localizes at the vacuole, and the localization depends on the interaction of Ivy1p with phosphoinositides and the small GTPase Ypt7 (Arlt *et al.*, 2011; Lazar *et al.*, 2002; Numrich *et al.*, 2015). These observations might suggest that the cellular protrusions in multicellular organisms share some characteristics with vacuole, one of the largest intracellular membrane compartments.

At present, five mammalian I-BAR proteins, IRSp53/BAIAP2, IRTKS/BAIAP2L1, PinkBAR/BAIAP2L2, MIM/MTSS1, and ABBA/MTSS1L (Scita *et al.*, 2008), have been identified. However, none of them has been reported as being localized at an intracellular membrane. Therefore, it is interesting that Ivy1p was localized at the intracellular membrane in HeLa cells, as shown in Fig. 5, suggesting that some other hidden I-BAR-like proteins function in forming the intracellular membranes of mammalian cells.

The formation of BAR domain polymers was reported in several BAR and F-BAR proteins, such as FBP17, CIP4, and endophilin (Frost *et al.*, 2008, 2009; Itoh *et al.*, 2005; Shimada *et al.*, 2007). These polymers were considered to be formed on the lipid membrane. Without the lipid membrane, the polymer of the BAR domain alone was observed by electron microscopy (Itoh *et al.*, 2005). However, this observation was not associated with the gelation of the protein, and thus the polymer formation may require some supportive materials, such as the collodion film (a kind of plastic) used for the preparation of electron microscopy sample grids. Recently, the formation of an Ivy1p polymer on the surface of giant liposomes was reported (Numrich *et al.*, 2015). In this study, we showed that Ivy1p polymerizes without any membrane support. The diameter of the Ivy1p filaments was approximately 20 nm, which is similar to the length of the longer axis of the I-BAR domains of IRSp53, Pinkbar/BAIAP2L2, and MIM, which are approximately 18–20 nm (Pykalainen *et al.*, 2011). It is still possible that the N- and/or C-terminal regions of Ivy1p are required for filament formation, because we could not purify the Ivy1p

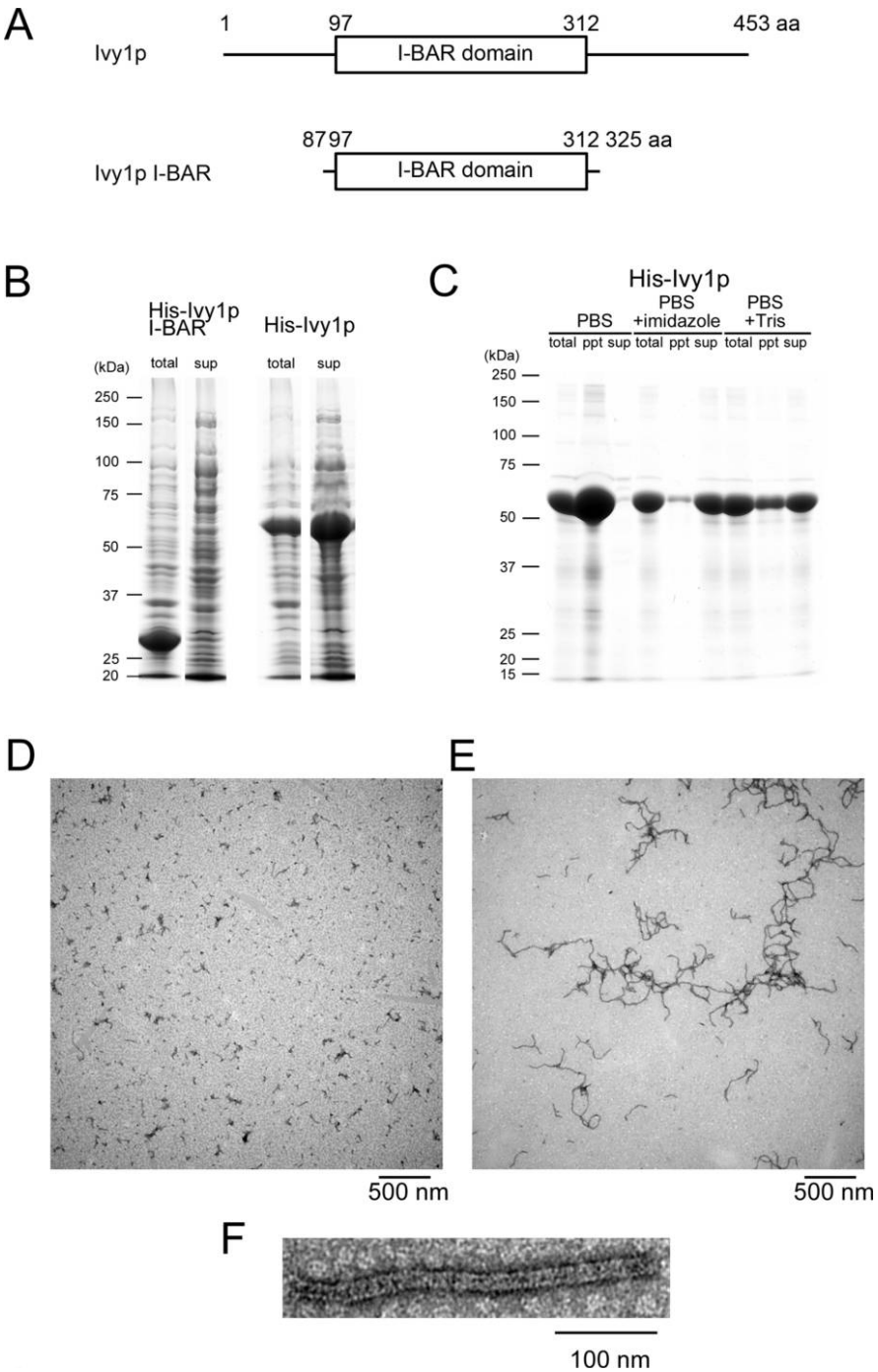

Fig. 4. Formation of Ivy1p polymers *in vitro*. (A) Domain compositions of the full-length and I-BAR-domain containing fragment of Ivy1p used in this study. (B) Solubility of Ivy1p. The His_6-tagged I-BAR-domain containing fragment and full-length Ivy1p were expressed in *E. coli*, and the solubility of the proteins in the lysate was analyzed. The total lysate and the supernatant of the lysate were monitored by SDS-PAGE. (C) Gelation of the purified Ivy1p. The gelled Ivy1p was generated by dialyzing the purified protein against PBS. The gelled Ivy1p precipitate after centrifugation was re-suspended in PBS containing 0.6 M imidazole or 0.1 M Tris (the final pH values are 9.0 and 9.5, respectively), and analyzed again by centrifugation. The supernatant (sup) and precipitate (ppt) of the sample were analyzed by SDS-PAGE. (D) Negative-stained images of soluble Ivy1p. The purified Ivy1p before dialysis was suspended in 10 mM Tris without pH adjustment. (E) Negative-stained images of filamentous Ivy1p. The purified Ivy1p was suspended in PBS. (F) Higher magnification images of Ivy1p filaments.

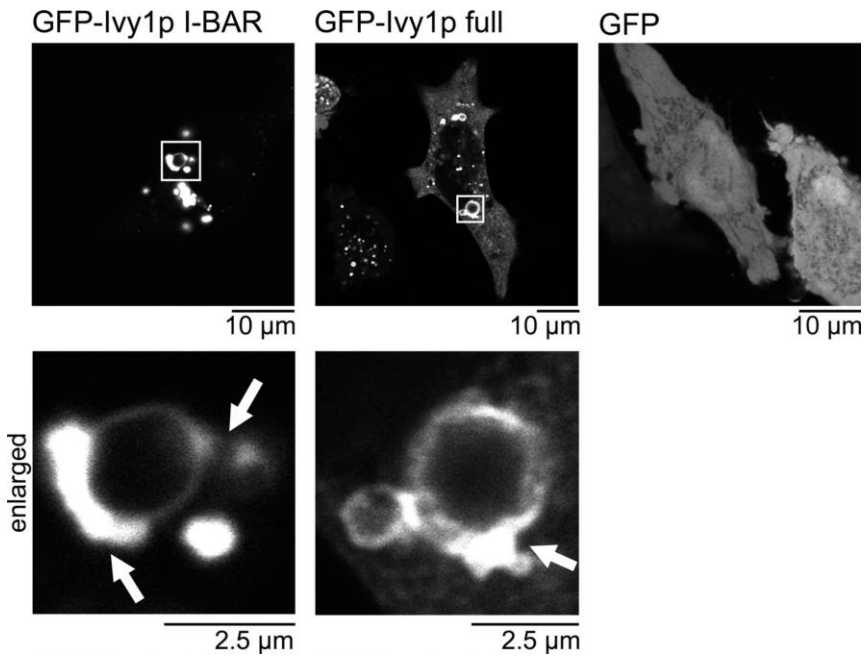

Fig. 5. Localization of Ivy1p in HeLa cells. The cellular localization of GFP-Ivy1p, GFP-Ivy1p-I-BAR, and GFP in HeLa cells, 24 hrs after transfection. The localization was observed by GFP fluorescence using confocal microscopy.

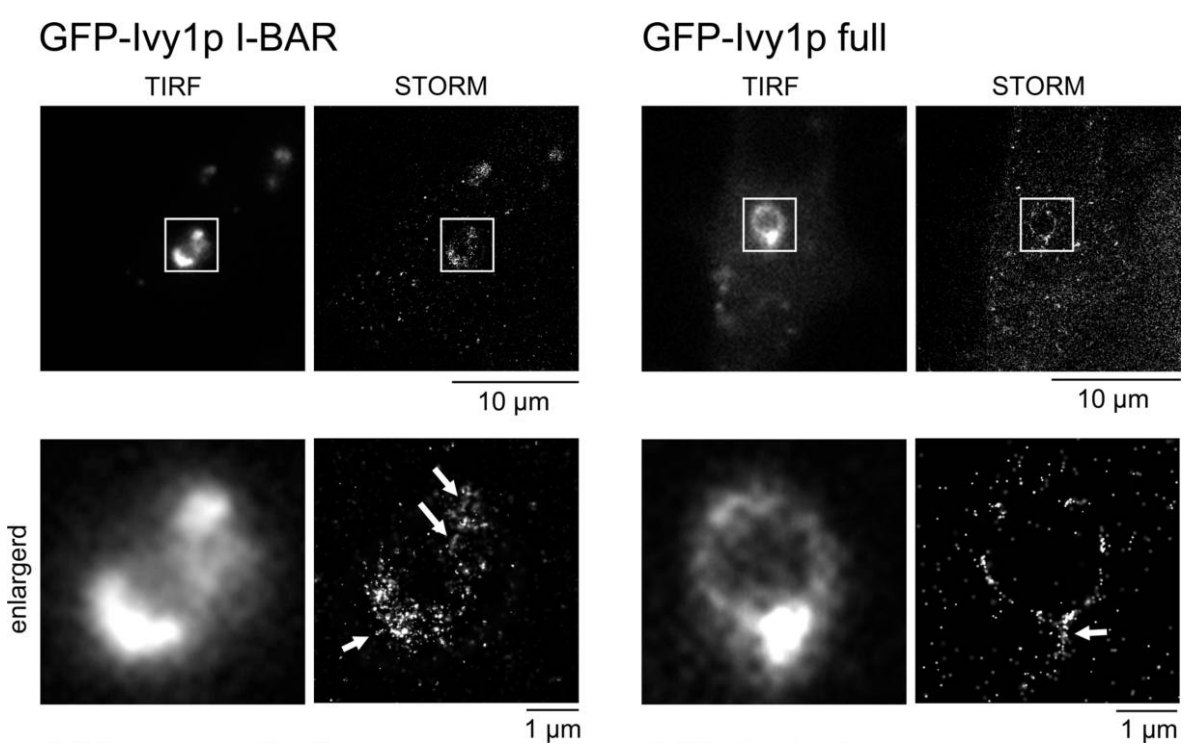

Fig. 6. Localization of Ivy1p in HeLa cells using super resolution microscopy. The cellular localization of GFP-Ivy1p and GFP-Ivy1p-I-BAR in HeLa cells, 24 hrs after transfection were observed by total internal reflection microscopy (TIRF) followed by super-resolution microscopy (STORM).

I-BAR domain alone. However, the STORM observation strongly indicates the filament forming ability of the I-BAR domain fragment (Fig. 6), and thus the inability to purify the I-BAR domain is supposed to be due to strong ability to form the filaments, which could be insoluble.

In this study, we found that the filament formation of Ivy1p depends on pH, where neutralization from basic condition induces filament formation whereas basic condition disassembles the filaments. Currently, it is totally unclear on the cellular role of the pH-dependent filament formation of Ivy1p. Because Ivy1p appears to be localized at cytoplasmic surface of vacuole, the environmental pH surrounding Ivy1p is considered to be neutral, though the actual pH around vacuole was unclear. It is possible that if vacuole raptures and the pH around vacuole might change, where acidification of the cytosol might induce the formation of Ivy1p filaments. Taken together, this study opens the possibility that some BAR proteins may function as polymer filaments that associate with intracellular membrane systems.

Acknowledgments. We thank Drs Yohei Katoh, and Kazuhisa Nakayama at Kyoto University for GFP nanobody plasmids. This work was supported by grants from the Funding Program for Next Generation World-Leading Researchers (NEXT program) and JSPS KAKENHI Grant Number 26291037 to S.S.

References

Adl, S.M., Simpson, A.G., Lane, C.E., Lukes, J., Bass, D., Bowser, S.S., Brown, M.W., Burki, F., Dunthorn, M., Hampl, V., Heiss, A., Hoppenrath, M., Lara, E., Le Gall, L., Lynn, D.H., McManus, H., Mitchell, E.A., Mozley-Stanridge, S.E., Parfrey, L.W., Pawlowski, J., Rueckert, S., Shadwick, R.S., Schoch, C.L., Smirnov, A., and Spiegel, F.W. 2012. The revised classification of eukaryotes. *J. Eukaryot. Microbiol.*, **59**: 429–493.

Altschul, S.F., Madden, T.L., Schäffer, A.A., Zhang, J., Zhang, Z., Miller, W., and Lipman, D.J. 1997. Gapped BLAST and PSI-BLAST: a new generation of protein database search programs. *Nucleic Acids Res.*, **25**: 3389–3402.

Arlt, H., Perz, A., and Ungermann, C. 2011. An overexpression screen in Saccharomyces cerevisiae identifies novel genes that affect endocytic protein trafficking. *Traffic (Copenhagen, Denmark)*, **12**: 1592–1603.

Bates, M., Huang, B., Dempsey, G.T., and Zhuang, X. 2007. Multicolor super-resolution imaging with photo-switchable fluorescent probes. *Science*, **317**: 1749–1753.

Buchan, D.W., Minneci, F., Nugent, T.C., Bryson, K., and Jones, D.T. 2013. Scalable web services for the PSIPRED Protein Analysis Workbench. *Nucleic Acids Res.*, **41**: W349–357.

Cavalier-Smith, T. 2009. Megaphylogeny, cell body plans, adaptive zones: causes and timing of eukaryote basal radiations. *J. Eukaryot. Microbiol.*, **56**: 26–33.

Daumke, O., Roux, A., and Haucke, V. 2014. BAR domain scaffolds in dynamin-mediated membrane fission. *Cell*, **156**: 882–892.

Doherty, G.J. and McMahon, H.T. 2008. Mediation, modulation, and consequences of membrane-cytoskeleton interactions. *Annu. Rev. Biophys.*, **37**: 65–95.

Fairclough, S.R., Chen, Z., Kramer, E., Zeng, Q., Young, S., Robertson, H.M., Begovic, E., Richter, D.J., Russ, C., and Westbrook, M.J. 2013. Premetazoan genome evolution and the regulation of cell differentiation in the choanoflagellate Salpingoeca rosetta. *Genome Biol.*, **14**: R15.

Frost, A., Perera, R., Roux, A., Spasov, K., Destaing, O., Egelman, E.H., De Camilli, P., and Unger, V.M. 2008. Structural basis of membrane invagination by F-BAR domains. *Cell*, **132**: 807–817.

Frost, A., Unger, V.M., and De Camilli, P. 2009. The BAR domain superfamily: membrane-molding macromolecules. *Cell*, **137**: 191–196.

Guerrier, S., Coutinho-Budd, J., Sassa, T., Gresset, A., Jordan, N.V., Chen, K., Jin, W.L., Frost, A., and Polleux, F. 2009. The F-BAR domain of srGAP2 induces membrane protrusions required for neuronal migration and morphogenesis. *Cell*, **138**: 990–1004.

Huang, B., Wang, W., Bates, M., and Zhuang, X. 2008. Three-dimensional super-resolution imaging by stochastic optical reconstruction microscopy. *Science*, **319**: 810–813.

Itoh, T., Erdmann, K.S., Roux, A., Habermann, B., Werner, H., and De Camilli, P. 2005. Dynamin and the actin cytoskeleton cooperatively regulate plasma membrane invagination by BAR and F-BAR proteins. *Dev. Cell*, **9**: 791–804.

Katoh, Y., Nozaki, S., Hartanto, D., Miyano, R., and Nakayama, K. 2015. Architectures of multisubunit complexes revealed by a visible immunoprecipitation assay using fluorescent fusion proteins. *J. Cell Sci.*, **128**: 2351–2362.

Larkin, M.A., Blackshields, G., Brown, N.P., Chenna, R., McGettigan, P.A., McWilliam, H., Valentin, F., Wallace, I.M., Wilm, A., Lopez, R., Thompson, J.D., Gibson, T.J., and Higgins, D.G. 2007. Clustal W and Clustal X version 2.0. *Bioinformatics*, **23**: 2947–2948.

Lazar, T., Scheglmann, D., and Gallwitz, D. 2002. A novel phospholipid-binding protein from the yeast Saccharomyces cerevisiae with dual binding specificities for the transport GTPase Ypt7p and the Sec1-related Vps33p. *Eur. J. Cell Biol.*, **81**: 635–646.

Lee, S.H., Kerff, F., Chereau, D., Ferron, F., Klug, A., and Dominguez, R. 2007. Structural basis for the actin-binding function of missing-in-metastasis. *Structure (London, England: 1993)*, **15**: 145–155.

Letunic, I., Doerks, T., and Bork, P. 2015. SMART: recent updates, new developments and status in 2015. *Nucleic Acids Res.*, **43**: D257–260.

Lin, Z., Sriskanthadevan, S., Huang, H., Siu, C.H., and Yang, D. 2006. Solution structures of the adhesion molecule DdCAD-1 reveal new insights into Ca(2+)-dependent cell-cell adhesion. *Nat. Struct. Mol. Biol.*, **13**: 1016–1022.

Linkner, J., Witte, G., Zhao, H., Junemann, A., Nordholz, B., Runge-Wollmann, P., Lappalainen, P., and Faix, J. 2014. The inverse BAR domain protein IBARa drives membrane remodeling to control osmoregulation, phagocytosis and cytokinesis. *J. Cell Sci.*, **127**: 1279–1292.

Maddison, D.R., Schulz, K.-S., and Maddison, W.P. 2007. The tree of life web project. *Zootaxa*, **1668**: 19–40.

Maddison, D. and Schulz, K.-S. 2009. The tree of life web project. 2007. URL: http://tolweborg

Marchler-Bauer, A., Derbyshire, M.K., Gonzales, N.R., Lu, S., Chitsaz, F., Geer, L.Y., Geer, R.C., He, J., Gwadz, M., Hurwitz, D.I., Lanczycki, C.J., Lu, F., Marchler, G.H., Song, J.S., Thanki, N., Wang, Z., Yamashita, R.A., Zhang, D., Zheng, C., and Bryant, S.H. 2015. CDD: NCBI's conserved domain database. *Nucleic Acids Res.*, **43**: D222–226.

Mattila, P.K., Pykalainen, A., Saarikangas, J., Paavilainen, V.O., Vihinen, H., Jokitalo, E., and Lappalainen, P. 2007. Missing-in-metastasis and IRSp53 deform PI(4,5)P2-rich membranes by an inverse BAR domain-like mechanism. *J. Cell Biol.*, **176**: 953–964.

Millard, T.H., Dawson, J., and Machesky, L.M. 2007. Characterisation of IRTKS, a novel IRSp53/MIM family actin regulator with distinct filament bundling properties. *J. Cell Sci.*, **120**: 1663–1672.

Numrich, J., Peli-Gulli, M.P., Arlt, H., Sardu, A., Griffith, J., Levine, T., Engelbrecht-Vandre, S., Reggiori, F., De Virgilio, C., and Ungermann, C. 2015. The I-BAR protein Ivy1 is an effector of the Rab7 GTPase Ypt7 involved in vacuole membrane homeostasis. *J. Cell Sci.*, **128**: 2278–2292.

Paunola, E., Mattila, P.K., and Lappalainen, P. 2002. WH2 domain: a small, versatile adapter for actin monomers. *FEBS Lett.*, **513**: 92–97.

Pykalainen, A., Boczkowska, M., Zhao, H., Saarikangas, J., Rebowski, G., Jansen, M., Hakanen, J., Koskela, E.V., Peranen, J., Vihinen, H., Jokitalo, E., Salminen, M., Ikonen, E., Dominguez, R., and Lappalainen, P. 2011. Pinkbar is an epithelial-specific BAR domain protein that generates planar membrane structures. *Nat. Struct. Mol. Biol.*, **18**: 902–907.

Ries, J., Kaplan, C., Platonova, E., Eghlidi, H., and Ewers, H. 2012. A simple, versatile method for GFP-based super-resolution microscopy via nanobodies. *Nat. Methods*, **9**: 582–584.

Saarikangas, J., Zhao, H., Pykalainen, A., Laurinmaki, P., Mattila, P.K., Kinnunen, P.K., Butcher, S.J., and Lappalainen, P. 2009. Molecular mechanisms of membrane deformation by I-BAR domain proteins. *Curr. Biol.*, **19**: 95–107.

Scita, G., Confalonieri, S., Lappalainen, P., and Suetsugu, S. 2008. IRSp53: crossing the road of membrane and actin dynamics in the formation of membrane protrusions. *Trends Cell Biol.*, **18**: 52–60.

Senju, Y., Itoh, Y., Takano, K., Hamada, S., and Suetsugu, S. 2011. Essential role of PACSIN2/syndapin-II in caveolae membrane sculpting. *J. Cell Sci.*, **124**: 2032–2040.

Shalchian-Tabrizi, K., Minge, M.A., Espelund, M., Orr, R., Ruden, T., Jakobsen, K.S., and Cavalier-Smith, T. 2008. Multigene phylogeny of choanozoa and the origin of animals. *PLoS ONE*, **3**: e2098.

Shimada, A., Niwa, H., Tsujita, K., Suetsugu, S., Nitta, K., Hanawa-Suetsugu, K., Akasaka, R., Nishino, Y., Toyama, M., Chen, L., Liu, Z.J., Wang, B.C., Yamamoto, M., Terada, T., Miyazawa, A., Tanaka, A., Sugano, S., Shirouzu, M., Nagayama, K., Takenawa, T., and Yokoyama, S. 2007. Curved EFC/F-BAR-domain dimers are joined end to end into a filament for membrane invagination in endocytosis. *Cell*, **129**: 761–772.

Suetsugu, S., Murayama, K., Sakamoto, A., Hanawa-Suetsugu, K., Seto, A., Oikawa, T., Mishima, C., Shirouzu, M., Takenawa, T., and Yokoyama, S. 2006. The RAC binding domain/IRSp53-MIM homology domain of IRSp53 induces RAC-dependent membrane deformation. *J. Biol. Chem.*, **281**: 35347–35358.

Suetsugu, S. and Gautreau, A. 2012. Synergistic BAR-NPF interactions in actin-driven membrane remodeling. *Trends Cell Biol.*, **22**: 141–150.

Suetsugu, S., Kurisu, S., and Takenawa, T. 2014. Dynamic shaping of cellular membranes by phospholipids and membrane-deforming proteins. *Phys. Rev.*, **94**: 1219–1248.

Suga, H., Chen, Z., de Mendoza, A., Sebé-Pedrós, A., Brown, M.W., Kramer, E., Carr, M., Kerner, P., Vervoort, M., and Sánchez-Pons, N. 2013. The Capsaspora genome reveals a complex unicellular prehistory of animals. *Nat. Commun.*, **4**: 2325.

Takenawa, T. and Suetsugu, S. 2007. The WASP-WAVE protein network: connecting the membrane to the cytoskeleton. *Nat. Rev. Mol. Cell Biol.*, **8**: 37–48.

Veltman, D.M., Auciello, G., Spence, H.J., Machesky, L.M., Rappoport, J.Z., and Insall, R.H. 2011. Functional analysis of Dictyostelium IBARa reveals a conserved role of the I-BAR domain in endocytosis. *Biochem. J.*, **436**: 45–52.

(Received for publication, November 10, 2015, accepted, December 2, 2015 and published online, December 9, 2015)